Simple Route to Gradient Concentric Metal and Metal Oxide Rings

Suck Won Hong,[†] Supratim Giri,[‡] Victor S.-Y. Lin,[‡] and Zhiqun Lin*,[†]

Department of Materials Science and Engineering and Department of Chemsitry, Iowa State University, Ames, Iowa 50011

Received August 9, 2006
Revised Manuscript Received September 25, 2006

The use of spontaneous self-assembly as a lithography- and external fields-free means to construct well-ordered, often intriguing structures has received much attention as a result of the ease of producing complex structures with small feature sizes. Self-assembly via irreversible solvent evaporation of a droplet containing nonvolatile solutes (polymers, nanoparticles, and colloids) represents one such case.[1−6] Recently, self-organized gradient concentric ring patterns have been produced by constraining a drop of polymer solution in a confined geometry composed of either two cylindrical mica surfaces placed at a right angle to one another or a sphere on a flat surface.[7−9] Rather than allowing the solvent to evaporate over the entire droplet area as in the traditional approach, in which droplets evaporate from a single surface,[1−3] the evaporation is restricted at the droplet edges.[7−9] The concentric rings are formed by controlled, repetitive pinning and depinning of the contact line (i.e., "stick−slip" motion).[7−9]

Ring structures have some unique features compared to their linear counterpart of the same size. For example, persistent currents can be induced by magnetic fields in conducting rings.[10] The ability to produce ring structures consisting of metals has been demonstrated on many occasions. Mesoscopic gold rings have been prepared via filling the porous membrane with a solution of gold precursor followed by calcination.[10,11] Highly ordered honeycomb-structured gold nanoparticle films with both circular and ellipitic pores have been fabricated in the presence of moist air flowing across the surface of the solution.[12] However, to the best of our knowledge, no well-ordered *concentric* rings (i.e., multi-rings) based on metal and metal oxide have been reported. The rings organized in a *concentric* mode many offer possibilities for many applications, including annular Bragg resonators for advanced optical communications systems.[13]

Herein, we report on a *simple* route to concentric rings of metals or metal oxide. The gradient concentric polymer rings with unprecedented regularity were self-organized on metal- (or metal oxide-) coated Si substrate via the evaporation-induced dynamic self-assembly of polymer in a confined geometry (Figure 1a). Subsequently, the rings were utilized as templates for the preparation of ordered metal or metal oxide rings by removing metal or metal oxide between polymer rings, followed by eliminating polymer rings as depicted in Figure 2. This method is fast and cost-effective, dispensing with the need for lithography and external electric fields. Moreover, there is no restriction on metal and metal oxide materials that can be used for the formation of concentric rings.

A thick layer of gold (Au; 45 nm), aluminum (Al; 1 μm), or titania (TiO_2; 140 nm) was thermally deposited on Si substrates. To ensure good adhesion between Au (or Al) and Si, a 2-nm-thick TiO_2 was first evaporated on Si substrates. To construct a sphere-on-Si geometry inside a chamber, a spherical lens made from fused silica with a radius of ∼1 cm and an abovementioned metal- (or metal oxide-) coated Si were used. Both the sphere and Si were firmly fixed at the top and the bottom of sample holders in the chamber, respectively. To implement a confined geometry, an inchworm motor with a step motion of a few micrometers was used to place the upper sphere into contact with the lower stationary Si substrate. Before they contacted (i.e., separated by approximately a few hundred micrometers apart), 23 μL of poly(methyl methacrylate) (PMMA; number average molecular weight, $M_n = 534$ kg/mol, and polydispersity, PDI $= 1.57$) in toluene solution ($c = 0.25$ mg/mL on Au-coated Si and $c = 1.0$ mg/mL on Al- and TiO_2-coated Si) was loaded and trapped within the gap between the sphere and Si as a result of the capillary force. The sphere was finally brought into contact with Si substrate by the inchworm motor such that a capillary-held PMMA solution forms with evaporation rate highest at the extremity as schematically illustrated in Figure 1a.

The evaporation of toluene at the capillary edge simply triggered the pinning of the contact line (i.e., "stick" and forming the first ring).[1] This led to an outward flow that carried nonvolatile PMMA to the edge.[1] During the deposition of PMMA, the initial contact angle of the capillary edge decreased gradually due to the evaporative volume loss of toluene to a critical angle at which the capillary force (depinning force) becomes larger than the pinning force.[9] This caused the jump of the contact line (i.e., "slip") to a new position at which a new ring developed.[3,8,9] Repetitive deposition and recession cycles of the contact line in the sphere-on-Si geometry resulted in the formation of periodic

* To whom correspondence should be addressed. E-mail: zqlin@iastate.edu.
[†] Department of Materials Science and Engineering.
[‡] Department of Chemistry.

(1) Deegan, R. D.; Bakajin, O.; Dupont, T. F.; Huber, G.; Nagel, S. R.; Witten, T. A. *Nature* **1997**, *389*, 827.
(2) Karthaus, O.; Grasjo, L.; Maruyama, N.; Shimomura, M. *Chaos* **1999**, *9*, 308.
(3) Adachi, E.; Dimitrov, A. S.; Nagayama, K. *Langmuir* **1995**, *11*, 1057.
(4) Rabani, E.; Reichman, D. R.; Geissler, P. L.; Brus, L. E. *Nature* **2003**, *426*, 271.
(5) Yabu, H.; Shimomura, M. *Adv. Funct. Mater.* **2005**, *15*, 575.
(6) Bigioni, T. P.; Lin, X. M.; Nguyen, T. T.; Corwin, E. I.; Witten, T. A.; Jaeger, H. M. *Nat. Mater.* **2006**, *5*, 265.
(7) Lin, Z. Q.; Granick, S. *J. Am. Chem. Soc.* **2005**, *127*, 2816.
(8) Hong, S. W.; Xu, J.; Xia, J.; Lin, Z. Q.; Qiu, F.; Yang, Y. L. *Chem. Mater.* **2005**, *17*, 6223.
(9) Xu, J.; Xia, J.; Hong, S. W.; Lin, Z. Q.; Qiu, F.; Yang, Y. L. *Phys. Rev. Lett.* **2006**, *96*, 066104.
(10) Yan, F.; Goedel, W. A. *Angew. Chem., Int. Ed.* **2005**, *44*, 2084.
(11) Yan, F.; Goedel, W. A. *Nano Lett.* **2004**, *4*, 1193.
(12) Li, J.; Peng, J.; Huang, W.; Wu, Y.; Fu, J.; Cong, Y.; Xue, L.; Han, Y. *Langmuir* **2005**, *21*, 2017.
(13) Scheuer, J.; Green, W. M. J.; Yariv, A. *Photonics Spectra* **2005** (May).

10.1021/cm0618805 CCC: $33.50
Published on Web 10/06/2006

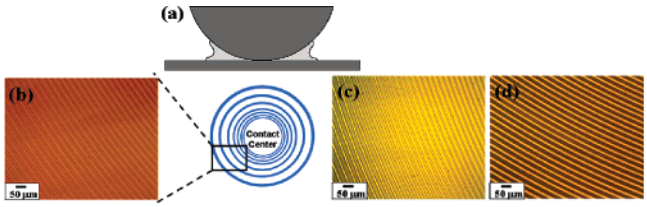

Figure 1. (a) Schematic cross section of a capillary-held solution containing nonvolatile solute placed in a sphere-on-Si geometry. (b) Schematic representation of gradient concentric rings of PMMA formed during solvent evaporation in the geometry shown in part a. The sphere/Si contact area is marked as "Contact Center". The optical micrograph of PMMA rings formed on the Au-coated Si surface is shown on the left side. (c, d) Optical micrographs of PMMA rings after dissolving Au between the rings (c), followed by subsequent removal of PMMA (d). The scale bar is 50 μm.

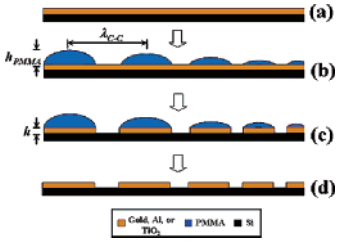

Figure 2. Schematic illustration of the formation of gradient concentric metal or metal oxide rings (cross-sectional view). (a) A layer of metal or metal oxide was evaporated on the Si surface. (b) Evaporation-induced self-assembly of PMMA rings from PMMA toluene solution, showing a decrease in the center-to-center distance between adjacent rings, λ_{C-C}, and the height of the ring, h_{PMMA}, from the outermost ring (left) toward the "Contact Center" (right).[9] (c) Removal of metal or metal between PMMA rings with a selective solution (e.g., KI/I_2 for Au removal). (d) Formation of metal or metal oxide rings upon removal of PMMA with acetone.

concentric rings of PMMA (left panel in Figure 1b in which a Au-coated Si substrate was used; see snapshots in Supporting Information, Figure 1S). The center to center distance, λ_{C-C}, between PMMA rings (left panel in Figure 1b) and height of the ring, h, decreased with increased proximity to the center of the sphere/Si contact (i.e., contact center in Figure 1b), attributing to the competition between linear pinning force and nonlinear capillary force.[9] It is noteworthy that to form a periodic family of concentric ring patterns of PMMA, the solvent evaporation must be homogeneous. This was realized by applying a symmetric geometry (sphere-on-Si) in conjunction with the use of a sealed chamber that eliminates the hydrodynamic instabilities and convection[14,15] over the course of solvent evaporation. Thus, as opposed to a stochastic "stick−slip" motion that was responsible for the formation of irregular rings,[3] the ring patterns of PMMA with unprecedented regularity were deposited on both sphere and Si surfaces. Only patterns formed on the Si surface were evaluated (left panel in Figure 1b). It is of interest to note that the gradient concentric ring patterns described here were highly reproducible.

The periodic organization of PMMA rings makes them an intriguing template for producing metal and metal oxide rings as schematically illustrated in Figure 2. PMMA rings formed at the surface of metal- or metal oxide-coated Si (Figure 2b) were treated with a selective solution to remove the metal or metal oxide layer between PMMA rings (Figure 2c). Subsequently, the sample was rinsed with acetone thoroughly to remove PMMA, thereby exposing underlying metal or metal oxide (Figure 2d), replicating the gradient feature of PMMA rings in terms of λ_{C-C}. The optical micrographs of PMMA rings on the Au-coated Si surface, PMMA rings after treatment with KI/I_2 mixed solution to remove Au between adjacent rings, and Au rings formed (i.e., exposed) after final removal of PMMA on their top with excessive acetone are shown in Figure 1b (left panel), Figure 1c, and Figure 1d, respectively. The order of Au rings (Figure 1d) was reminiscent of the arrangement of PMMA rings (left panel in Figure 1b) and was not disrupted during the successive eliminations of Au and PMMA (Figure 1c,d). The integrity (i.e., shape and size) of Au rings (Figure 1d) was unchanged in comparison to that of the PMMA rings (left panel in Figure 1b).

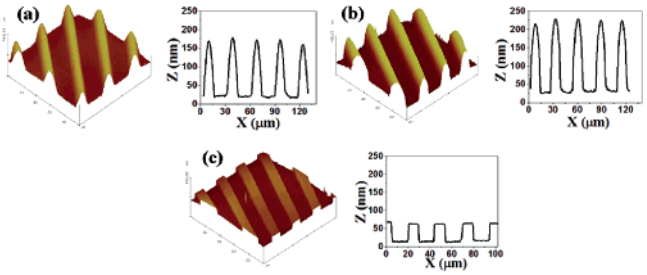

Figure 3. AFM images of rings (i.e., stripes locally; left) and corresponding profiles (right). (a) PMMA rings formed on a Au-coated Si surface via controlled, repetitive "stick−slip" motion of the contact line ($c = 0.25$ mg/mL). (b) PMMA rings after removal of Au between adjacent PMMA rings with KI/I_2 mixed solution. (c) Au rings obtained after completely rinsing PMMA off with excessive acetone. These images correspond to the stages shown in Figure 1b−d, respectively. The image size is 100 × 100 μm^2.

To verify the accessibility of the sequence demonstrated in optical micrographs (Figure 1b−d; corresponding to the steps in Figure 2b−d), atomic force microscopy (AFM) measurements were performed. Figure 3 shows three-dimensional (3D) AFM height images (left) and the corresponding cross sections taken perpendicular to the rings (right). Locally, the rings appeared as the stripes. The height of the PMMA ring on the Au-coated Si substrate, h_{PMMA}, is ∼155 nm (Figure 3a). The width of the ring, w, is ∼13.2 μm, and the center-to-center distance between adjacent rings, λ_{C-C}, is ∼27.7 μm. Upon selective removal of Au, the height of the stripe is expected to increase. The section analysis of the AFM image yields $h + h_{PMMA} \sim 199$ nm, $w \sim 13.5$ μm, and $\lambda_{C-C} \sim 27.8$ μm, respectively (Figure 3b). Thus, the thickness of Au, h, is 44 nm. This is in excellent agreement with the value obtained after removing PMMA on the top of buried Au ($h \sim 45$ nm from Figure 3c). Rather than humplike stripes (Figure 3a,b), stepwise stripes are clearly evident (Figure 3c). It should be noted that lower values of w (∼11.7 μm) and λ_{C-C} (∼24.8 μm) were found in Figure 3c, owing to the AFM image taken at the location that was closer to the center of sphere/Si contact than those in Figure 3a,b.

The gradient concentric Au sample was then reacted with 25 μL of 6-FAM-Q-labeled (green emitting fluorescent dye; 6-FAM-Q: 1-dimethoxytrityloxy-3-[*O*-(*N*-carboxy-(di-*O*-pivaloyl-fluorescein)-3-aminopropyl)]-propyl-2-*O*-succinoyl−long chain alkylamino-CPG) thiolated oligonucleotides (pur-

(14) Maillard, M.; Motte, L.; Ngo, A. T.; Pileni, M. P. *J. Phys. Chem. B* **2000**, *104*, 11871.
(15) Nguyen, V. X.; Stebe, K. J. *Phys. Rev. Lett.* **2002**, *88*, 164501.

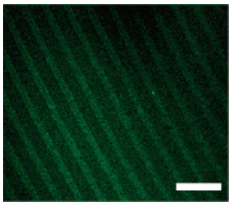

Figure 4. Fluorescence image of 6-FAM-Q-labeled thiolated oligonucleotide patterns formed on Au rings. The scale bar is 100 μm.

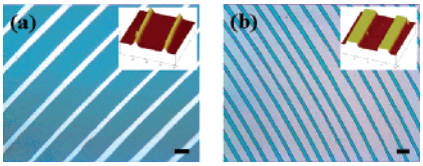

Figure 5. Optical micrographs of gradient concentric rings of (a) Al and (b) TiO_2. The scale bar is 20 μm in part a and 50 μm in part b, respectively. Representative 3D AFM images (80 × 80 μm^2) are given as insets. The *z* scale is 1 μm in part a and 400 nm in part b. The concentration of PMMA toluene solution used to produce PMMA rings is $c = 1$ mg/mL.

chased from Operon Biotechnologies, Inc.) deionized (DI) water solution. A cover glass was placed on the top of the Au sample sealed with a poly(dimethylsiloxane) gasket to prevent water evaporation. Subsequently, the sample was put in a humidified chamber for 24 h. The absorption and emission maxima of the green-emitting dye 6-FAM-Q are 494 and 520 nm, respectively. As a result, Au rings were modified with oligonucleotides through the formation of the Au−S bond (Figure 4), emitting green fluorescence. The oligonucleotide-deposited Au surface was rinsed with DI water to wash away unbonded oligonucleotide. The thickness of oligonucleotide adsorbed on Au rings was 7 nm, determined by AFM. The oligonucleotides adsorbed physically on Si surfaces (between Au rings) also caused fluorescence but were much weaker. In the future, an extensive rinse with a phosphate-buffered solution will be conducted, and the PH of the solution and the rinsing time will be optimized to achieve a clear fluorescence image exclusively on the Au rings.[16]

To demonstrate that a wide variety of metals or metal oxides can be used to make rings in gradient concentric mode, Al and TiO_2 (semiconductor) coated Si substrates were employed. TiO_2 possesses the highest known dielectric constant of the oxide materials that renders a variety of applications in electronics, optics, and solar cells.[17] Figure 5 shows optical micrographs of Al rings and TiO_2 rings created in a manner similar to the process of preparing Au rings. Al and TiO_2 between PMMA rings were selectively removed with 20 wt % potassium hydroxide (KOH) DI water solution for 2 min and 5 vol % hydrofluoric acid (HF) DI water solution for less than 1 min, respectively. Finally, PMMA rings were completely rinsed off with acetone, thereby exposing Al and TiO_2 underneath. The heights of the Al and TiO_2 rings are 410 and 140 nm shown in Figure 5a,b, respectively. Representative 3D AFM height images are shown in Figure 5a,b as insets, respectively. The λ_{C-C} of the metal and semiconductor rings can be easily tuned by varying the concentration of the PMMA toluene solution.[8,9] A larger λ_{C-C} is clearly evident due to the use of the PMMA toluene solution with a higher concentration ($c = 1$ mg/mL; Figure 5) as compared to the 0.25 mg/mL solution used for preparing Au rings (Figure 1b−d).[9] The height of the rings is mainly dictated by the thickness of the metal and semiconductor sputtered on the Si substrates prior to drying-mediated self-assembly of PMMA rings as seen in Au and TiO_2 rings, possessing a smooth ring surface (Figure 3c and the inset in Figure 5b). However, in the first step of preparation of Al rings, due to fast reaction of Al and KOH, Al between the PMMA rings (see schematic in Figure 2b,c) was removed very quickly. In the meantime, partial dissolution of intact Al underneath PMMA rings occurred, thereby reducing the width and the height of intact Al. Consequently, humplike Al rings were obtained (inset in Figure 5a).

In conclusion, a rational construction of simple sphere-on-flat geometry provides remarkable control and flexibility over the preparation of gradient concentric rings of nonvolatile solutes produced by repeated "stick−slip" motion of the contact line. This simple, lithography-free route allows subsequent preparation of a great variety of metal and metal oxide concentric ring patterns with controlled spacing, size, and thickness. The utilization of such a gradient replica to engineer biopolymers (i.e., oligonucleotides) has been demonstrated. We envision that, owing to intrinsic gradient nature in spacing and width together with well-controlled physical and chemical surface properties, metal and metal oxide rings may provide the basis for combinatorial study of dewetting of polymer thin films,[18] phase separation of polymer blends[19] as well as polymer/liquid crystal mixtures,[20] and long range ordering of block copolymers[21] to explore finite size (i.e., confinement) effects in *one step*. These rings may also be employed as unique surfaces for studying the confinement of transmembrane cell receptors[22] and the biological recognition process.[23]

Acknowledgment. This work was supported by the 3M Nontenured Faculty Award, the American Chemical Society Petroleum Research Fund (Grant 42825-G7), and the University Research Grant (URG) at Iowa State University (Z.L. and S.W.H.). V.S.Y.L. and S.G. thank U.S. National Science Foundation (NSF) CHE-0239570 and CMS-0409625 for financial support.

Supporting Information Available: Snapshots of evaporation-induced dynamic self-assembly of PMMA (PDF). This material is available free of charge via the Internet at http://pubs.acs.org.

CM0618805

(16) Matsumoto, F.; Harada, M.; Nishio, K.; Masuda, H. *Adv. Mater.* **2005**, *17*, 1609.
(17) Mor, G. K.; Shankar, K.; Paulose, M.; Varghese, O. K.; Grimes, C. A. *Nano Lett.* **2006**, *6*, 215−218.
(18) Kargupta, K.; Sharma, A. *Phys. Rev. Lett.* **2001**, *86*, 4536.
(19) Böltau, M.; Walheim, S.; Mlynek, J.; Krausch, G.; Steiner, U. *Nature* **1998**, *391*, 877.
(20) Xia, J. F.; Wang, J.; Lin, Z. Q.; Qiu, F.; Yang, Y. L. *Macromolecules* **2006**, *39*, 2247.
(21) Kim, S. H.; Minser, M. J.; Xu, T.; Kimura, M.; Russell, T. P. *Adv. Mater.* **2004**, *16*, 226.
(22) Purrucker, O.; Fortig, A.; Ludtke, K.; Jordan, R.; Tanaka, M. *J. Am. Chem. Soc.* **2005**, *127*, 1258.
(23) Delamarche, E.; Bernard, A.; Schmid, H.; Michel, B.; Biebuyck, H. *Science* **1997**, *276*, 779.